



Using the Freescale MMA9550L for High Resolution Spectral Estimation of Vibration Data

by: Mark Pedley

1 Introduction

This technical note examines the suitability of the Freescale MMA9550L Intelligent Motion-Sensing Platform for high resolution, real-time, spectral analysis of vibration data for engine monitoring and failure prediction.

This note covers i) the architecture of the MMA9550L ii) the mathematics of the Discrete Fourier Transform (DFT) iii) results from applying the DFT to vibration time series containing amplitude modulation, phase modulation and impulsive noise and iv) example MMA9550L C code with calculations of memory footprint and processing overhead.

Full technical documentation for the MMA9550L may be found on the Freescale website www.freescale.com by entering a search for part number 'MMA9550L'.

Contents

1	Introduction	1
1.1	Key Words	2
1.2	Summary	2
2	Freescale MMA9550L Architecture	2
2.1	Single Axis Discrete Fourier Transform	2
2.2	3-Axis Discrete Fourier Transform	4
2.3	Advantages and Limitations of the Fast Fourier Transform Algorithm	4
2.4	Modeling Engine Vibration	5
2.5	Simulation Results	6
2.6	MMA9550L Software and Benchmarking	9

1.1 Key Words

MMA9550L, DFT, FFT, Vibration, Spectral Analysis, Amplitude Modulation, Phase Modulation, Impulsive Noise.

1.2 Summary

1. Abnormal operating conditions, indicating developing wear or possible imminent failure, can manifest as characteristic signals in the vibration spectrum of the machinery.
2. The vibration spectrum can be computed by direct evaluation of the DFT or by using the FFT algorithm. It is shown that the FFT algorithm adds a significant overhead in memory use and produces only a minor reduction in computation when only a limited number of vibration frequencies are of interest.
3. Calculation of the DFT in no more than 16 frequency bins is shown to be effective at determining the characteristic features of amplitude modulation, phase modulation and impulsive noise present in vibration data measured by the MMA9550L's accelerometer.
4. Reference C code shows that the MMA9550L is capable of computing 16 DFT bins from all three accelerometer channels, in real time at kHz rates, and is ideally suited for this application.

2 Freescale MMA9550L Architecture

Freescale's MMA9550L integrates a 3-axis 8-bit to 14-bit MEMS accelerometer, an 8 MHz 32-bit Coldfire processor core, 16 KB flash memory and 2 KB SRAM into a single 3 mm by 3 mm 16 pin package drawing less than 5 mW power. The MMA9550L is targeted towards applications requiring processing of accelerometer data at low cost and low power. The MMA9550L communicates with an external processor over a 2 Mbps slave I²C bus or via an interrupt pin.

The MMA9550L accelerometer is configurable to operate in $\pm 2g$, $\pm 4g$ and $\pm 8g$ modes with 8-bit to 14-bits resolution at sampling rates up to 3.9 kHz. A 400 kbps master I²C interface allows additional accelerometers or other sensors to be interfaced to the MMA9550L.

2.1 Single Axis Discrete Fourier Transform

The Discrete Fourier Transform (DFT) $X(\omega)$ of the N point sampled accelerometer x -axis data series $I[]$ at normalized angular frequency ω (or frequency f in Hz) is:

$$X(\omega) = \sum_{n=0}^{N-1} x[n]e^{-i\omega n} \quad \text{Eqn. 1}$$

$$X(f) = \sum_{n=0}^{N-1} x[n]e^{-\left(\frac{2\pi ifn}{f_s}\right)} \quad \text{Eqn. 2}$$

ω and f are related through the sampling frequency f_s by:

$$\omega = \frac{2\pi f}{f_s} \quad \text{Eqn. 3}$$

ω and f are limited between the negative and positive Nyquist frequencies:

$$-\pi < \omega \leq \pi \quad \text{Eqn. 4}$$

$$-\left(\frac{f_s}{2}\right) < f \leq \left(\frac{f_s}{2}\right) \quad \text{Eqn. 5}$$

The frequency resolution achievable from a time series of N data points improves proportionally to N and it is common practice to evaluate the DFT $X[k]$ at N equally spaced normalized angular frequency bins $\omega[k]$:

$$\omega[k] = \frac{2\pi k}{N} \quad \text{Eqn. 6}$$

$$X[k] = \sum_{n=0}^{N-1} x[n] e^{-j\left(\frac{2\pi i k n}{N}\right)} \quad \text{Eqn. 7}$$

$$-\frac{N}{2} < k \leq \frac{N}{2} \quad \text{Eqn. 8}$$

The range of k in Equation 8 does not include $k = \frac{-N}{2}$ since it is easily verified that $X\left[\frac{-N}{2}\right] = X\left[\frac{N}{2}\right]$.

The value of the DFT for vibration analysis is that frequencies present in the time series $x[n]$ are transformed into peaks at the appropriate DFT frequency bin. Specifically, if $x[n]$ is a complex sinusoid with amplitude $a[l]$ and normalized angular frequency $\omega[l] = \frac{2\pi l}{N}$ then:

$$x[n] = a[l] e^{j\left(\frac{2\pi i l n}{N}\right)} \quad \text{Eqn. 9}$$

$$X[k] = [k] = \sum_{n=0}^{N-1} x[n] e^{-j\left(\frac{2\pi i k n}{N}\right)} = a[l] \sum_{n=0}^{N-1} e^{j\left(\frac{2\pi i (l-k)n}{N}\right)} \quad \text{Eqn. 10}$$

For $k = l$, Equation 10 simplifies to:

$$X[l] = Na[l] \quad \text{Eqn. 11}$$

For $k \neq l$, equation 10 is the sum of a geometric progression which evaluates to zero:

$$X[k] = \frac{\{1 - e^{2\pi i(l-k)}\}}{\left\{1 - e^{\left(\frac{2\pi i(l-k)}{N}\right)}\right\}} = 0 \quad \text{Eqn. 12}$$

A sinusoid at normalized angular frequency $\omega[l]$ therefore manifests as a peak of value $N\alpha[l]$ in bin l of the DFT with all other bins zero. Since the DFT is a linear operator, an input time series comprising the sum of sinusoids of multiple frequencies has a DFT with peaks at those frequencies with magnitude proportional to those of the component sinusoids. The magnitude squared of the DFT is commonly referred to as the "power spectrum" of the input time series.

2.2 3-Axis Discrete Fourier Transform

Equation 1 can be readily extended to compute the DFTs $Y(\omega)$ and $Z(\omega)$ of the two other accelerometer data series $y[]$ and $z[]$.

The DFT amplitude $A(\omega)$ of the combined spectrum from all three accelerometer channels can be computed from the DFTs of the individual channels. Vibration frequencies present in any of the three accelerometer channels appear without distortion in the three-axis amplitude $A(\omega)$:

$$A(\omega) = \sqrt{\{X(\omega)\}^2 + \{Y(\omega)\}^2 + \{Z(\omega)\}^2} \quad \text{Eqn. 13}$$

The DFT should not be computed from the modulus $a[n]$ of the three axes of acceleration signals. The acceleration time series $a[n]$ is non-negative resulting in harmonic distortion and the appearance of DFT peaks at integer multiples of the original frequencies.

$$\alpha[n] = \sqrt{x[n]^2 + y[n]^2 + z[n]^2} \quad \text{Eqn. 14}$$

2.3 Advantages and Limitations of the Fast Fourier Transform Algorithm

The computational complexity of the DFT in Equation 7 is quadratic in N since it involves the summation over N data points to compute the DFT in N frequency bins. The Fast Fourier Transform (FFT) algorithm is an extremely efficient algorithm to compute the DFT over the N equally spaced bins of Equation 7 with computational complexity proportional to $N \log_2 N$. Even for small data series of $N = 1024 = 2^{10}$ points, the saving is $\frac{2^{10}}{\log_2(2^{10})} \approx 100$. For million point FFTs $N = 1048576 = 2^{20}$ the computational saving from using the FFT algorithm is $\frac{2^{20}}{\log_2(2^{20})} \approx 50000$. The FFT algorithm is therefore unarguably superior in computational efficiency compared to direct calculation of the DFT provided that the DFT is required at all N frequency bins.

If the DFT is required at a lower number of frequency bins M , where $M < N$, then the FFT algorithm may not be the most efficient. Specifically, direct calculation of the DFT will be more efficient for $M < \log_2 N$ which for $N = 1024$ data points occurs at $M = 10$ frequency bins.

The FFT algorithm is efficient in using working memory since the algorithm over-writes the N input data points with the N output data points. However, an N point FFT still requires storage of N complex values each of which, in fixed point systems, typically consists of two 32-bit integers or 8 bytes per bin and $8N$ bytes storage in total.

In contrast, the DFT calculation of M frequency bins requires $8M$ bytes for the complex DFT bin plus (as will be seen later) $8M$ bytes for phasor storage totaling $16M$ bytes. This $16M$ byte storage requirement for direct DFT calculation is independent of the number of points N used in the calculation which is a major advantage over the FFT for long data sequences.

Assuming that 256 bytes per accelerometer channel of the 2 KB working RAM in the MMA9550L is available for spectral estimation, then the FFT algorithm is limited to just $256/8 = 32$ input data points and 32 frequency bins. At a sampling rate of 2 kHz, the spectral resolution is just $2000/32 = 62$ Hz.

In contrast, the use of the DFT on a sample by sample basis using the same 256 bytes of storage allows the calculation of the spectrum at $16M = 256$ or $M = 16$ unique frequency points using an arbitrary number of accelerometer readings which in turn leads to arbitrary high spectral resolution. The 16 available frequency bins may be positioned uniformly within ± 1 Hz of a frequency component giving a DFT resolution of just 0.125 Hz. $8s \times 2 \text{ kHz} = 16000$ accelerometer measurements will be required to achieve that frequency resolution but this does not increase the storage requirement.

Using the FFT algorithm with the same 2 kHz sampling frequency, this same resolution requires the storage of all $8s \times 2 \text{ kHz} = 16000$ accelerometer measurements. This is not remotely feasible for the MMA9550L nor other low cost embedded processors.

The $M = 16$ available frequency bins for direct sample by sample DFT calculation will normally be i) located in the immediate vicinity of the fundamental to provide high resolution analysis and also ii) at multiples of the machinery fundamental for broad band analysis. These situations are examined in more detailed in the remainder of this technical note.

2.4 Modeling Engine Vibration

This section contains the results of modeling various sources of vibration disturbance on rotating machinery and demonstrates the ability to compute their characteristics using only a small number of DFT bins.

A well-balanced and stable machine operating at frequency f_0 will create a small level of vibration at frequency f_0 only. Increasing engine wear and loss of stability will, however:

- a) increase the magnitude of the vibration at frequency f_0
- b) decrease the stability of the engine rotation
- c) introduce once per rotation cycle perturbations (one example being 'knocking' in internal combustion engines)

A simple mathematical model represents the vibration in one accelerometer axis $x[n]$ by:

$$x[n] = A \left\{ 1 + \varepsilon \cos\left(\frac{2\pi f_M n}{f_s}\right) \right\} \cos\left(\frac{2\pi f_0 n}{f_s} + \psi[n]\right) + B \sum_{j=-\infty}^{\infty} \delta\left[j - \frac{f_0 n}{f_s}\right] \tag{Eqn. 15}$$

The machinery vibration fundamental has amplitude A at frequency f_0 with amplitude modulation with depth δ at frequency f_M .

$\psi[n]$ is phase modulation noise modelled as a sinusoidally varying phase error of defined frequency and amplitude.

The final term is a Dirac comb function which comprises an infinite number of delta functions $\delta[\cdot]$ centered at intervals of $\frac{f_s}{f_0}$ samples and which represents repetitive impulsive noise with amplitude B .

Simple Fourier analysis predicts that:

- a) amplitude modulation will split the DFT peak at the fundamental frequency f_0
- b) phase modulation will broaden the DFT peak at the fundamental frequency f_0
- c) impulse noise occurring once per cycle will create peaks in the DFT at integer multiples of the fundamental frequency f_0 .

The next section shows that these predicted signatures can be determined using just a limited number of DFT bins.

2.5 Simulation Results

The simulations in this section used a sampling frequency f_s of 2 kHz and an engine fundamental frequency f_0 equal to 244 Hz. The fundamental vibration amplitude A was 64 bits. 5s or 10,000 data points were analyzed into the fundamental plus 10 narrow band frequency bins and 3 broad band frequency bins.

Figure 1 shows a narrow band DFT computed in 11 bins between 243 Hz and 245 Hz in the absence of any additional distortions. The DFT resolution of 0.2 Hz is matched to the 5s duration of the data analyzed. Only the vibration of the engine fundamental appears in the DFT.

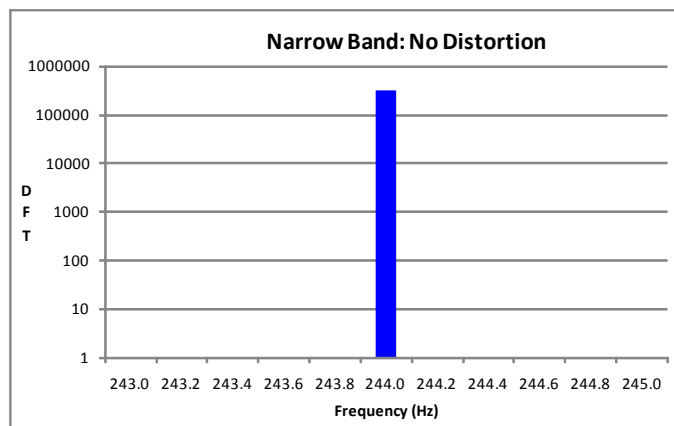


Figure 1. Narrow Band DFT with no distortion

Figure 2 shows the narrow band DFT but in the presence of amplitude modulation of the fundamental frequency with 0.6 Hz modulation frequency and modulation amplitude equal to 0.1%. The amplitude modulation is clearly resolved by peaks separated from the fundamental by 0.6 Hz.

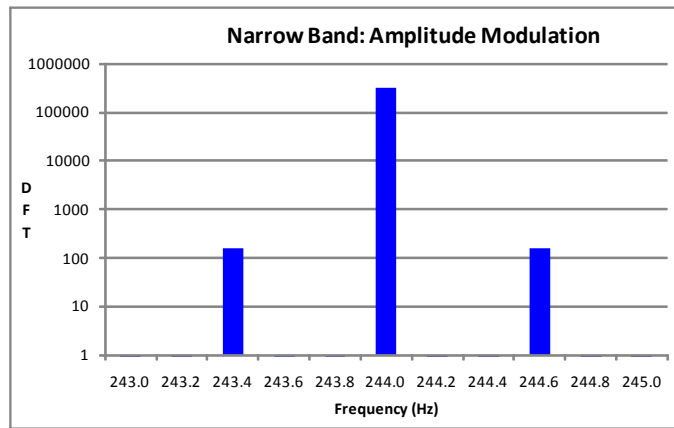


Figure 2. Narrow Band DFT with amplitude modulation

Figure 3 shows the narrow band DFT in the presence of a sinusoidally varying phase error with modulation frequency of 0.1 Hz and amplitude of 0.01 radians. The broadening of the fundamental peak is clearly visible indicating loss of frequency stability.

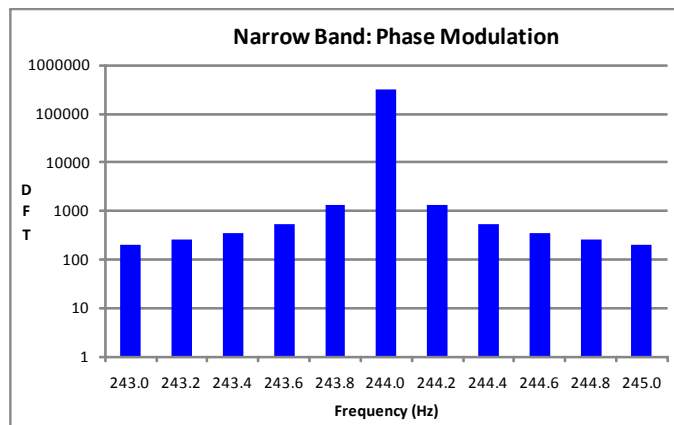


Figure 3. Narrow Band DFT with Phase Modulation

Figure 4 shows the DFT computed at the engine fundamental frequency and at three harmonics of the fundamental. In the absence of distortion, there is no DFT energy at the higher harmonics.

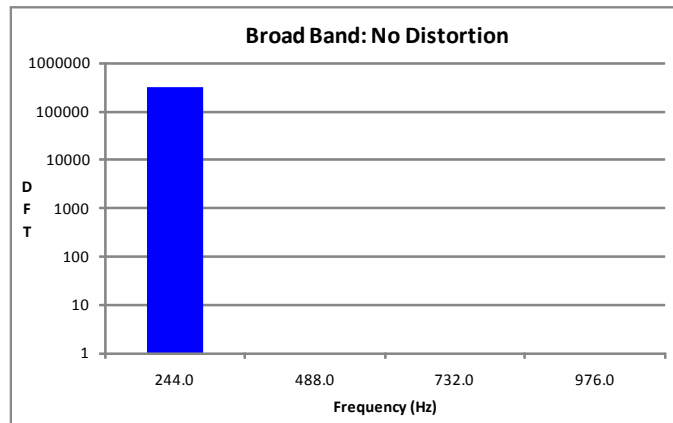


Figure 4. Broad Band DFT with no distortion

Figure 5 shows the same DFT but in the presence of repetitive impulse noise with amplitude 1 bit occurring once per cycle of the fundamental. The impulse noise is readily detectable at the harmonics of the fundamental frequency.

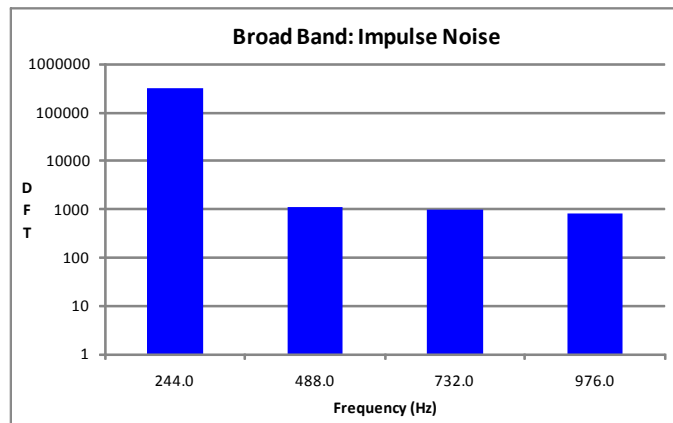


Figure 5. Broad Band DFT with repetitive impulse noise

The conclusion of this section is that calculation of the DFT at a limited number of bins can detect engine vibration disturbances of the different types discussed. The frequencies of the DFT bins to be computed are readily determined from the engine fundamental frequency.

2.6 MMA9550L Software and Benchmarking

It is highly inefficient to compute the complex phasor in Equation 2 though calls to trigonometric functions. An alternative and efficient iterative approach updates the phasor $\phi[f, n]$ for frequency f at data sample n by rotating the phasor $\phi[f, n - 1]$ from the previous sample by the constant rotation angle phasor $\phi[f, 1]$:

$$\phi[f, 0] = 1 \quad \text{Eqn. 16}$$

$$\phi[f, 1] = e^{\frac{(-2\pi if)}{f_s}} \quad \text{Eqn. 17}$$

$$\phi[f, n] = e^{-\frac{(2\pi if)}{f_s}} = e^{-\frac{(2\pi if(n-1))}{f_s}} e^{-\frac{(2\pi if)}{f_s}} = \phi[f, n-1]\phi[f, 1] \quad \text{Eqn. 18}$$

The rotation phasor $\phi[f, 1] = e^{\frac{(-2\pi if)}{f_s}}$ is a constant which defines the DFT frequency of interest and only needs calculation once either i) by the MMA9550L from the required frequency f or, more likely, ii) computed and downloaded to the MMA9550L by an external processor at initialization of the MMA9550L.

Equation 2 can now be implemented in a recursive algorithm as:

$$X(f, 0) = x[0] \quad \text{Eqn. 19}$$

$$X(f, n) = X(f, n + 1) + x[n]\phi[f, n] \quad \text{Eqn. 20}$$

The key code kernel which executes once per sample for the computation of NBINS DFT bins from a single accelerometer channel the vibration data sample $x[n]$ is listed below.

The compile time constant SCALING is application dependent and should be set to prevent overflow for the typical vibration amplitude measured and the length of the accelerometer time series used in the summation.

The real and imaginary components of the rotation phasor are stored in Q15 integer format where -32768 represents -1.000 and +32767 represents 0.9999.

```

INT16 RePhasor1[NBINS];/* array of real parts of rotation phasor Phi(f,1) */
INT16 ImPhasor1[NBINS];/* array of imaginary parts of rotation phasor Phi(f,1) */
INT16 RePhasorN[NBINS];/* array of real parts of rotation phasor Phi(f,n) */
INT16 ImPhasorN[NBINS];/* array of imaginary part of rotation phasor Phi(f,n) */
INT32 ReDFT[NBINS];/* array of real parts of DFT bins */
INT32 ImDFT[NBINS];/* array of imaginary parts of DFT bins */
INT16 temp; /* temporary register */
INT16 xn; /* current accelerometer sample from one channel */
INT16 i; /* loop counter */

/* loop over all frequency bins where the DFT is to be computed */
for (i = 0; i < NBINS; i++)
{

```

```

/* update the DFT bin for sample xn using the current frequency phasor */
ReDFT[i] += (xn * RePhasorn[i]) >> SCALING;
ImDFT[i] += (xn * ImPhasorn[i]) >> SCALING;
/* update the frequency phasor for the next iteration */
temp = RePhasorn[i];
RePhasorn[i] = (INT16) ((RePhasorn[i] * RePhasor1[i] - ImPhasorn[i] * ImPhasor1[i]) >> 15);
ImPhasorn[i] = (INT16) ((temp * ImPhasor1[i] + ImPhasorn[i] * RePhasor1[i]) >> 15);
}

```

Four INT16s and two INT32s (totaling 16 bytes) are required for each DFT frequency bin resulting in $16M$ bytes of RAM storage per accelerometer channel for calculation of M DFT frequency bins. This is an extremely small RAM footprint permitting $M = 16$ DFT frequencies to be computed for all three accelerometer channels using just $3 \times 16 \times 16 = 768$ bytes of the MMA9550L's 2KB internal RAM. The RAM storage requirement is completely independent of the number of accelerometer data points analyzed.

The code kernel above requires just 10 arithmetic operations per accelerometer sample per DFT bin per accelerometer channel. At sampling frequency f_s and with NBINS DFT frequencies computed, the arithmetic processing rate for all three accelerometer channels is $10 \times 3 \times \text{NBINS} \times f_s$ or $480 f_s$ operations per second for NBINS = 16. For $f_s = 2 \text{ kHz}$ this totals 1M arithmetic operations per second, well within the processing capability of the 8 MHz MMA9550L.

How to Reach Us:

Home Page:

www.freescale.com

Web Support:

<http://www.freescale.com/support>

USA/Europe or Locations Not Listed:

Freescale Semiconductor, Inc.
Technical Information Center, EL516
2100 East Elliot Road
Tempe, Arizona 85284
1-800-521-6274 or +1-480-768-2130
www.freescale.com/support

Europe, Middle East, and Africa:

Freescale Halbleiter Deutschland GmbH
Technical Information Center
Schatzbogen 7
81829 Muenchen, Germany
+44 1296 380 456 (English)
+46 8 52200080 (English)
+49 89 92103 559 (German)
+33 1 69 35 48 48 (French)
www.freescale.com/support

Japan:

Freescale Semiconductor Japan Ltd.
Headquarters
ARCO Tower 15F
1-8-1, Shimo-Meguro, Meguro-ku,
Tokyo 153-0064
Japan
0120 191014 or +81 3 5437 9125
support.japan@freescale.com

Asia/Pacific:

Freescale Semiconductor China Ltd.
Exchange Building 23F
No. 118 Jianguo Road
Chaoyang District
Beijing 100022
China
+86 10 5879 8000
support.asia@freescale.com

For Literature Requests Only:

Freescale Semiconductor Literature Distribution Center
1-800-441-2447 or +1-303-675-2140
Fax: +1-303-675-2150
LDCForFreescaleSemiconductor@hibbertgroup.com

Information in this document is provided solely to enable system and software implementers to use Freescale Semiconductor products. There are no express or implied copyright licenses granted hereunder to design or fabricate any integrated circuits or integrated circuits based on the information in this document.

Freescale Semiconductor reserves the right to make changes without further notice to any products herein. Freescale Semiconductor makes no warranty, representation or guarantee regarding the suitability of its products for any particular purpose, nor does Freescale Semiconductor assume any liability arising out of the application or use of any product or circuit, and specifically disclaims any and all liability, including without limitation consequential or incidental damages. "Typical" parameters that may be provided in Freescale Semiconductor data sheets and/or specifications can and do vary in different applications and actual performance may vary over time. All operating parameters, including "Typicals", must be validated for each customer application by customer's technical experts. Freescale Semiconductor does not convey any license under its patent rights nor the rights of others. Freescale Semiconductor products are not designed, intended, or authorized for use as components in systems intended for surgical implant into the body, or other applications intended to support or sustain life, or for any other application in which the failure of the Freescale Semiconductor product could create a situation where personal injury or death may occur. Should Buyer purchase or use Freescale Semiconductor products for any such unintended or unauthorized application, Buyer shall indemnify and hold Freescale Semiconductor and its officers, employees, subsidiaries, affiliates, and distributors harmless against all claims, costs, damages, and expenses, and reasonable attorney fees arising out of, directly or indirectly, any claim of personal injury or death associated with such unintended or unauthorized use, even if such claim alleges that Freescale Semiconductor was negligent regarding the design or manufacture of the part.

Freescale and the Freescale logo are trademarks of Freescale Semiconductor, Inc., Reg. U.S. Pat. & Tm. Off. The Energy Efficiency Solutions Logo and Xtrinsic are trademarks of Freescale Semiconductor, Inc.

All other product or service names are the property of their respective owners.

© 2012 Freescale Semiconductor, Inc. All rights reserved.